



**HAL**  
open science

# Evidence for Non-Monotonic and Broadband Electron Distributions in the Europa Footprint Tail Revealed by Juno In Situ Measurements

J. Rabia, V. Hue, J R Szalay, N. André, Q. Nénon, M. Blanc, F. Allegrini, S J Bolton, J E P Connerney, R W Ebert, et al.

## ► To cite this version:

J. Rabia, V. Hue, J R Szalay, N. André, Q. Nénon, et al.. Evidence for Non-Monotonic and Broadband Electron Distributions in the Europa Footprint Tail Revealed by Juno In Situ Measurements. *Geophysical Research Letters*, 2023, 50 (12), 10.1029/2023GL103131 . insu-04155050

**HAL Id: insu-04155050**

**<https://insu.hal.science/insu-04155050>**

Submitted on 7 Jul 2023

**HAL** is a multi-disciplinary open access archive for the deposit and dissemination of scientific research documents, whether they are published or not. The documents may come from teaching and research institutions in France or abroad, or from public or private research centers.

L'archive ouverte pluridisciplinaire **HAL**, est destinée au dépôt et à la diffusion de documents scientifiques de niveau recherche, publiés ou non, émanant des établissements d'enseignement et de recherche français ou étrangers, des laboratoires publics ou privés.



Distributed under a Creative Commons Attribution 4.0 International License

# Geophysical Research Letters<sup>®</sup>



## RESEARCH LETTER

10.1029/2023GL103131

### Key Points:

- Juno unambiguously observed 10 events of downward electron acceleration from Europa at various downtail separations with the moon
- Precipitating energy fluxes decrease exponentially as a function of downtail distance from the moon, with an e-folding of 7.4°
- Two types of electron distributions exist: non-monotonic in the near tail and broadband in the far tail

### Supporting Information:

Supporting Information may be found in the online version of this article.

### Correspondence to:

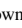







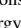


J. Rabia,  
[jonas.rabia@irap.omp.eu](mailto:jonas.rabia@irap.omp.eu)

### Citation:

Rabia, J., Hue, V., Szalay, J. R., André, N., Nénon, Q., Blanc, M., et al. (2023). Evidence for non-monotonic and broadband electron distributions in the Europa footprint tail revealed by Juno in situ measurements. *Geophysical Research Letters*, 50, e2023GL103131. <https://doi.org/10.1029/2023GL103131>

Received 3 FEB 2023  
Accepted 1 APR 2023

## Evidence for Non-Monotonic and Broadband Electron Distributions in the Europa Footprint Tail Revealed by Juno In Situ Measurements

J. Rabia<sup>1</sup> , V. Hue<sup>2,3</sup>, J. R. Szalay<sup>4</sup> , N. André<sup>1</sup> , Q. Nénon<sup>1</sup>, M. Blanc<sup>1,3</sup> , F. Allegrini<sup>2,5</sup>, S. J. Bolton<sup>2</sup> , J. E. P. Connerney<sup>6,7</sup> , R. W. Ebert<sup>2,5</sup> , G. R. Gladstone<sup>2,5</sup> , T. K. Greathouse<sup>2</sup>, P. Louarn<sup>1</sup> , A. Mura<sup>8</sup> , E. Penou<sup>1</sup>, and A. H. Sulaiman<sup>9</sup> 

<sup>1</sup>Institut de Recherche en Astrophysique et Planétologie, CNRS-UPS-CNES, Toulouse, France, <sup>2</sup>Southwest Research Institute, San Antonio, TX, USA, <sup>3</sup>LAM, Pythéas, Aix Marseille Université, CNRS, CNES, Marseille, France, <sup>4</sup>Department of Astrophysical Sciences, Princeton University, Princeton, NJ, USA, <sup>5</sup>Department of Physics and Astronomy, University of Texas at San Antonio, San Antonio, TX, USA, <sup>6</sup>NASA Goddard Space Flight Center, Greenbelt, MD, USA, <sup>7</sup>Space Research Corporation, Annapolis, MD, USA, <sup>8</sup>Institute for Space Astrophysics and Planetology, National Institute for Astrophysics, Rome, Italy, <sup>9</sup>School of Physics and Astronomy, Minnesota Institute for Astrophysics, University of Minnesota, Minneapolis, MN, USA

**Abstract** We characterize the precipitating electrons accelerated in the Europa-magnetosphere interaction by analyzing in situ measurements and remote sensing observations recorded during 10 crossings of the flux tubes connected to Europa's auroral footprint tail by Juno. The electron downward energy flux, ranging from 34 to 0.8 mW/m<sup>2</sup>, exhibits an exponential decay as a function of downtail distance, with an e-folding factor of 7.4°. Electrons are accelerated at energies between 0.3 and 25 keV, with a characteristic energy that decreases downtail. The electron distributions form non-monotonic spectra in the near tail (i.e., within an angular separation of less than 4°) that become broadband in the far tail. The size of the interaction region at the equator is estimated to be 4.2 ± 0.9 Europa radii, consistent with previous estimates based on theory and UV observations.

**Plain Language Summary** The space environment close to Jupiter is dominated by the magnetic field of the giant planet in a so-called magnetosphere. The four Galilean moons, including Europa, orbit deep inside the Jovian magnetosphere and therefore constantly interact with the rapidly rotating plasma flow made of charged particles trapped by the magnetic field of the giant planet. The interaction between moons and plasma generates electromagnetic waves, accelerate particles and produce emissions at various wavelengths, including bright UV auroral spots and tails in the atmosphere of Jupiter. In this work, we present 10 events where the Juno spacecraft observed both in situ and remotely the acceleration of electrons due to the interaction between the icy moon Europa and the magnetospheric environment. We characterize the properties of the accelerated electrons. In particular, we find that acceleration is maximum near the moon itself, and that two distinct families of electron distributions exist.

## 1. Introduction

Moon-magnetospheres interaction result from the encounter between a magnetospheric plasma flow and moons, which act as obstacles to the plasma flow. In the Jovian magnetosphere, the Galilean moons orbit with a Keplerian velocity much slower than the plasma velocity, driven in near corotation by the planetary magnetic field. This means that in the reference frame of the moons, the plasma flows with a relative velocity ranging from 57 km s<sup>-1</sup> for Io up to 192 km s<sup>-1</sup> for Callisto (Saur, 2021). Therefore, they disturb the magnetospheric plasma flow, which in turn generates Alfvén waves in their close environments. These waves propagate along the bent magnetic field lines, forming the so-called Alfvén wings, accelerating particles, and triggering auroral emissions in the giant planet atmosphere.

Thanks to decades of remote sensing, these moon-induced auroral emissions have been studied in various wavelengths, including infrared (Connerney et al., 1993), ultraviolet (UV) (Clarke et al., 1996; Prangé et al., 1996) and radio (Bigg, 1964; Zarka, 1998). The Io-magnetosphere interaction, which has the broadest and brightest signatures, has been the most studied one. Four features have been identified in the Io footprint revealing the

© 2023. The Authors.

This is an open access article under the terms of the [Creative Commons Attribution License](https://creativecommons.org/licenses/by/4.0/), which permits use, distribution and reproduction in any medium, provided the original work is properly cited.

complexity of the interaction: the Main Alfvén Wing (MAW) spot which is the brightest spot, the transhemispheric electrons beam (TEB) spot created by electrons accelerated in the opposite hemisphere, the Reflected Alfvén Wing (RAW) spot which is the reflection of the MAW, and an auroral tail (Bonfond et al., 2008). In the case of Europa, a spot multiplicity related to both MAW and RAW spots has been reported (Bonfond, Grodent, et al., 2017) as well as a footprint tail (Bonfond, Saur, et al., 2017).

Since August 2016, the Juno mission (Bolton et al., 2017) has made it possible to characterize in situ the moon-magnetosphere interactions near the polar regions as well as in the equatorial plane of the magnetosphere. Several crossings of the flux tubes connected to the orbits of the Galilean moons have been reported, revealing a diversity of particle properties and acceleration processes (Allegrini et al., 2020; Hue et al., 2022; Szalay et al., 2018, 2020a; Szalay, Bagenal, et al., 2020). Evidence for broadband, likely Alfvénic electron acceleration has been reported in the Io and Ganymede flux tubes (Szalay et al., 2020a; Szalay, Bagenal, et al., 2020), while electrostatic electron acceleration may occur in the Europa MAW spot (Allegrini et al., 2020). A multi-event study of the Io-magnetosphere interaction based on Juno data has revealed that the precipitating electron energy flux (EF) decreases exponentially with distance in the footprint tail (Szalay et al., 2020b). These measurements are consistent with the observed variation of the UV brightness of the Io auroral tail (Bonfond, Saur, et al., 2017; Hue et al., 2022).

However, the Europa-magnetosphere interaction, whose remote and in situ signatures are weaker and more difficult to identify than those of Io, remain poorly known. In the present paper, we extend the method presented by Szalay et al. (2020b) to the case of Europa. We identify 10 unambiguous crossings of the Europa footprint tail based on Juno in situ measurements and remote sensing observations, and characterize the properties of the corresponding downward electrons fluxes. To do so, we use a set of physical parameters derived from several Juno instruments as described in Section 2. Section 3 presents the results of our study. A discussion of these results is provided in Section 4. Finally, we draw the main conclusions and perspectives for future works in Section 5.

## 2. Instrument Description and Methodology

The electron measurements shown in the following section are obtained by the Jovian Auroral Distributions Experiment (JADE, McComas et al., 2017) onboard the Juno spacecraft. The electron sensors JADE-E consist of two identical electrostatic analyzers, with a  $120^\circ$  field of view, measuring electrons with energies ranging from 50 eV to 100 keV. The two instruments, when combined, provide a field of view of  $240^\circ$  which allows a partial or complete coverage in the pitch angle domain depending on the orientation of the spacecraft relative to the magnetic field. UV data are obtained by the Ultraviolet Spectrograph of Juno (UVS, Gladstone et al., 2017). The UVS instrument is a photon-counting imaging spectrograph operating between 68 and 210 nm dedicated to the study of the Jovian auroral emissions.

Thanks to its highly-elliptical polar orbit crossing magnetic shells (hereinafter denoted as M-shells) in the range  $M = 1$  to  $M > 70$ , Juno crosses the M-shell of all Galilean moons at least twice per orbit at various latitudes and angular separation with these moons. This unique observational data set witnesses the diversity of physical processes involved in moon-magnetosphere interactions. We study the 43 first orbits of the Juno mission, which represent nearly six years of data, from August 2016 to July 2022. For each perijove (PJ), we estimate the time at which Juno has intercepted magnetic flux tubes connected to Europa or its wake by computing the instantaneous footprint of the spacecraft on the Jupiter poles and tracking when it crossed Europa's auroral footprint. All of the computations related to the magnetic field, that is, M-Shell, position of the footprints and projection of the spacecraft trajectory on Jupiter's atmosphere, are made using the internal magnetic field model JRM33 (Connerney et al., 2022) combined with the CON2020 current sheet model (Connerney et al., 2020). We then compute the position of Juno's footprint (JFP) and of Europa's footprint (EFP) projected 400 km above the 1-bar surface level and select only the cases when Juno is magnetically downstream of Europa with respect to the plasma flow (i.e.,  $\Delta\lambda_{\text{Lon}} = \lambda_{\text{JFP}} - \lambda_{\text{EFP}} > 0$ , where  $\lambda$  are the longitudes of the footprints in System III Right Handed coordinate system). A criterion on Juno's altitude was also added to ensure that the JADE-E sensors are able to resolve the loss cone (LC) and efficiently deflect the field-aligned electrons to the inner part of the analyzer: we only consider crossings where Juno's altitude is lower than  $1.25 R_J$  ( $1 R_J = 71,492$  km). Altitude is computed as the distance above an ellipsoid whose polar and equatorial axis are 66,854 km and 71,492 km, respectively.

Twenty-six cases of potential crossings of Europa's magnetic shell by Juno have been identified with  $\Delta\lambda_{\text{Lon}}$  ranging from  $0^\circ$  to  $90^\circ$ . For each of these cases, we visually identify acceleration signatures in the Europa-magnetosphere

interaction by analyzing the JADE-E measurements in a 10-min interval centered on the estimated time of the crossing. We then correlate the sequence of events seen in the in situ measurements with the auroral emissions observed along the Juno footpath in the UVS data, as done in Figure 1 of Allegrini et al. (2020). From the corresponding catalog of 26-cases, only 10 signatures of the Europa-magnetosphere interaction have been unambiguously identified in the JADE-E data and confirmed by the UVS images. We do not consider any crossings with  $\Delta\lambda_{\text{Lon}} > 90^\circ$  because at this angular separation Europa's footprint is expected to be too faint to be seen in the UVS images, which prevents us from cross-identifying the Europa-magnetosphere signatures in the JADE-E and UVS data (Bonfond, Saur, et al., 2017).

To characterize the electron properties during each crossing, we compute a set of physical quantities that are calculated as follows. The EF is calculated using the formula from Mauk et al. (2017), that is,  $EF = \pi \sum_i DEF_i \times \Delta E_i$  where  $\pi$  represents the area of the LC projected on Jupiter's atmosphere, DEF refers to the Differential EF and  $\Delta E_i$  is the width of each energy bin. The characteristic energy of the electrons ( $E_c$ ) is defined as  $E_c = (\sum_i DNF_i \times E_{m,i} \times \Delta E_i) / (\sum_i DNF_i \times \Delta E_i)$  where DNF is the differential number flux (or intensity) and  $E_{m,i}$  the mean energy of each energy bin (Clark et al., 2018). To relate the electron properties to the footprint brightness in the Jovian upper atmosphere, computation of the EF is made using the DEF within the LC, when the pitch angle coverage allows it. The size of the LC is estimated by  $LC \approx \sin^{-1}(1/R^3)^{1/2}$  with  $R$  the joviocentric distance in  $R_J$  (Mauk et al., 2017) as done in Allegrini et al. (2020).

### 3. Results

Figure 1 shows the JADE-E and UVS observations for 5 of the 10 crossings for which we identify a clear signature of the Europa-magnetosphere interaction, including the perijove 12 North (PJ12N) already studied by Allegrini et al. (2020). The remaining JADE-E and UVS observations for the five other crossings are provided in the Supporting Information S1 (Figure S1) as well as time, position, and flux information for each crossing (Table S1 in Supporting Information S1).

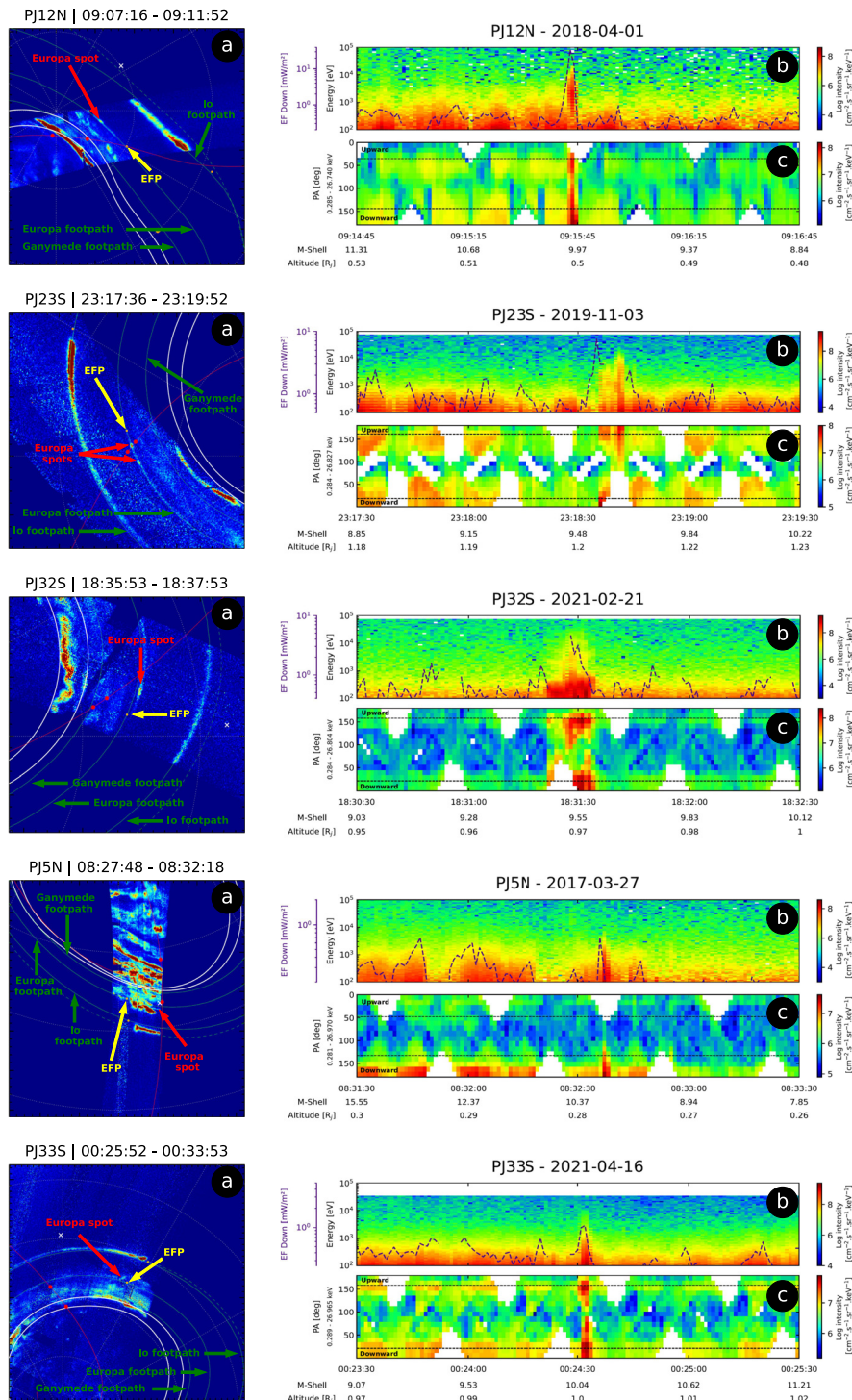
All signatures of acceleration in the Europa footprint tail identified in the JADE-E data and shown in Figure 1 and Figure S1 in Supporting Information S1 appear to have similar characteristics in terms of energy, time duration, and bidirectionality. First, the increase of the electron DNF, which delineates the crossing of Europa's flux tube, lasts for a few seconds (<15 s), indicating that the electrons accelerated during the Europa-magnetosphere interaction are very localized in space. Second, most of the accelerated electrons have an energy between 0.3 and 25 keV. We therefore compute the electron downward EF using this energy range. We point out that including the electrons with energies below 0.3 keV in the EF calculations increase the values by at most 1.6% for all measurements. Interestingly, the bidirectionality of the electron beams is observed most of the time, as predicted by Hess et al. (2010) in the case of an Alfvénic acceleration at Io.

For each event, the calculated downward electron EF is organized according to three metrics introduced by Szalay et al. (2020b). The first one,  $\Delta\lambda_{\text{Lon}}$ , only considers the difference in longitude (System III East) between the footprints of Juno and Europa. However, this metric does not take into account the fact that the Europa's footpath is not well centered on the jovigraphic pole, especially in the northern hemisphere. Two footprints with little separation in System III longitude may therefore be widely separated along the footpath (e.g., PJ29N in Figure 2a). To account for this difference, we consider the  $\Delta\lambda_{\text{Frac}}$  metric in which the separation between the footprints of Juno and Europa is calculated by integrating the distance along the Europa's footpath and dividing it by the total length of the footpath in each hemisphere. We multiply this fraction by  $360^\circ$  to have an angular separation ranging from  $0^\circ$  to  $360^\circ$ . Finally, the  $\Delta\lambda_{\text{Alfvén}}$  metric is the third one used. The angular separation between Europa and Juno is computed by numerically back-tracing the path of Alfvén waves from Juno's magnetic footprint to their previous position on the Europa's orbital plane. This calculation is based on an empirical model derived from the Juno UVS observations of Europa's MAW spot positions as a function of the position of the moon in the magnetodisk (Hue et al., 2023).

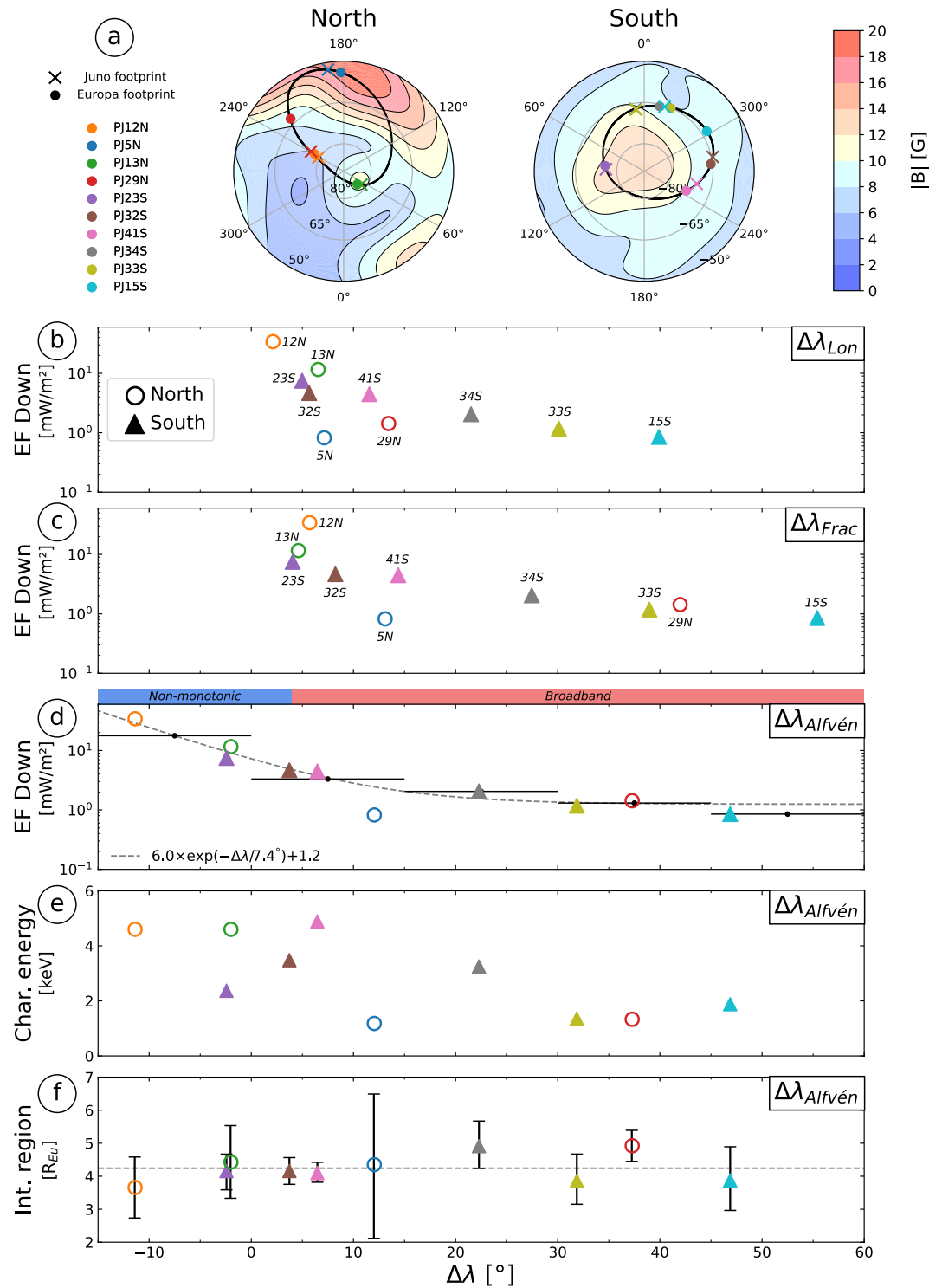
Figure 2a displays the location of the footprints of Juno and Europa on the northern and southern hemispheres overplotted onto the magnetic field strength on Jupiter's surface. Black curves highlight the statistical location of the Europa footprint calculated with JRM33 + CON2020 magnetic models.

Figures 2b–2d show the downward electron EF calculated for each event organized according to the  $\Delta\lambda_{\text{Lon}}$ ,  $\Delta\lambda_{\text{Frac}}$ , and  $\Delta\lambda_{\text{Alfvén}}$  metrics, respectively. In any case, the downward electron energy fluxes decrease with downtail

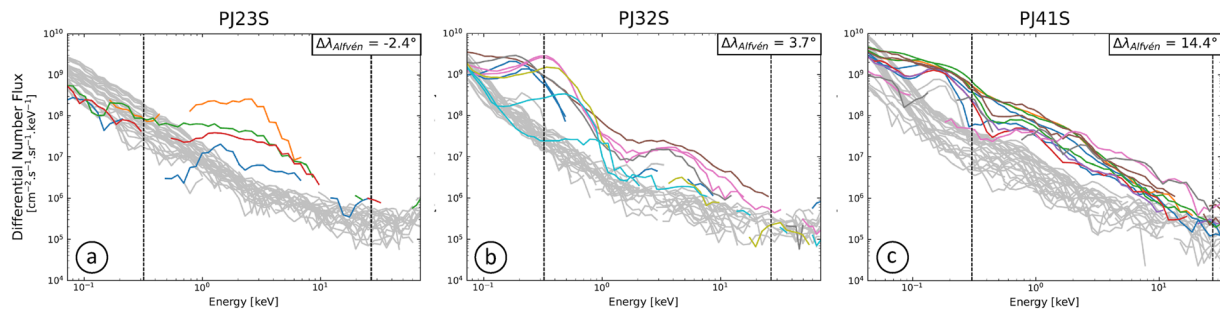




**Figure 1.** UV images and JADE-E spectrograms of 5 crossings of flux tubes connected to Europa's orbit: PJ12N, PJ23S, PJ32S, PJ5N, and PJ33S. The UVS observations recorded closest in time from the flux tube crossings as identified on JADE-E data are shown on panels (a). The time range over which these data were co-added, between 2 and 8 min, varies depending upon data availability. The red line indicates Juno's magnetic footprint projected at 400 km altitude, while the red dots, the orange dots and the green curves give the Juno's instantaneous footprint at the time of data acquisition, the footprints of the moons, and their projected footpaths, respectively. The white cross and dot, when displayed, indicate the sub-spacecraft point and the sub-solar longitude, respectively. The main auroral oval is delineated by the two solid white lines. Panels (b) show the electron DNF within the loss cone (LC) and the downward energy flux, depicted by the purple dashed lines. Panels (c) show the electron pitch angle distribution in the energy range indicated on the left axis. Black dotted lines give the estimated size of the LC at the time of the crossing.



**Figure 2.** (a) Location of the JFP and EFP superimposed onto the magnetic field intensity, calculated with the JRM33 model at Jupiter's 1-bar level. Panels (b–d) show the downward energy fluxes as a function of  $\Delta\lambda_{\text{Lon}}$ ,  $\Delta\lambda_{\text{Frac}}$ , and  $\Delta\lambda_{\text{Alfvén}}$  (see main text for definition of the three metrics). Circles and triangles refer to the hemisphere where Juno is located when the events are observed. Dashed gray line in panel (d) shows exponential least square fits with data averaged in  $15^\circ$  intervals. The black horizontal lines represent the  $\Delta\lambda_{\text{Alfvén}}$  intervals within which we average the energy fluxes, while the black dots indicate the mean EF in each  $\Delta\lambda_{\text{Alfvén}}$  interval. On top of panel (d), we report the type of electron distributions identified. Panels (e, f) display the electron characteristic energy and size of the equatorial interaction region derived from the JADE-E data as a function of the downtail distance, respectively. The dashed gray curve on panel (f) displays the  $4.2 R_{\text{Eu}}$  mean value.



**Figure 3.** DNF within the downward loss cone integrated over 1 s as a function of energy for 3 crossings (time intervals specified in Table S1 in Supporting Information S1): PJ23S, PJ32S, and PJ41S. The colored curves represent the DNF during the crossings while the gray curves show the DNF 15 s before and after the crossings. Vertical dashed lines delineate the energy ranges used to compute the downward energy flux and characteristic energy.

distance. The highest energy fluxes are measured in the near tail (i.e.,  $\Delta\lambda_{\text{Alfvén}} < 4^\circ$ ), up to  $34.1 \text{ mW/m}^2$  for the PJ12N event, while further down the tail the lowest value reaches  $0.85 \text{ mW/m}^2$  for the PJ15S. The flux measured during the PJ5N event is surprisingly low and outside of the global trend. We however note that the altitude of Juno during this crossing is the lowest of all the studied events. The presence of magnetospheric injections close to the Europa footprint (Figure 1a) might also explain this weak downward flux. Indeed, disappearance of the Io and Ganymede footprints in the presence of magnetospheric injections have been previously reported (Bonfond, Grodent, et al., 2017; Hess et al., 2013). In Figure 2a, injection events appear as bright and localized auroral spots. The distinction between injections and Europa footprints is made by looking at the rotation rate of their auroral signatures, which is close to plasma corotation for injections but follows the orbital motion of the moon in the case of a footprint.

The observed exponential law decay in the downward electron EF (Figures 2b–2d) is consistent with the two estimates provided by Bonfond, Saur, et al. (2017) who computed the e-folding using both the theoretical formalism of Hill and Vasylūnas (2002) and UV observations from the Hubble Space Telescope. These studies show that the tail brightness decays exponentially, with a theoretical e-folding value of  $6^\circ$  and an observational value of  $14^\circ$ . To compute our e-folding values, an exponential fit is made after averaging and re-binning the data in  $15^\circ$  intervals. Our calculations find an e-folding value of  $7.4^\circ$ , which is in good agreement with the previously stated values.

The electron characteristic energy also tends to decrease as Juno crossed the Europa flux tube further down in the tail (Figure 2e). The size of the interaction region in the equatorial plane was estimated by magnetically projecting the position of Juno onto Europa's orbital plane. By taking the difference between the radial distance on the equatorial plane at the beginning and at the end of the event, we found that the size of the interaction region is on average  $4.2 R_{\text{Eu}}$  ( $1 R_{\text{Eu}} = 1,560 \text{ km} = 1 \text{ Europa radius}$ ). Figure 2f shows these values as a function of the downtail extent. We derived an uncertainty of  $\pm 0.9 R_{\text{Eu}}$  on this result, considering that the uncertainties on the crossing time are  $\pm 1 \text{ s}$ . This value is in agreement with the one derived by Allegrini et al. (2020) during the PJ12N (i.e.,  $3.6 \pm 1 R_{\text{Eu}}$ ) and with the estimates based on UVS data, that is,  $< 6 R_{\text{Eu}}$  (Bonfond, Gladstone, et al., 2017). Furthermore, we note that the size of the interaction region observed by Juno in the far-field region is consistent with the radial extent of the perturbations modeled close to Europa itself by MHD and hybrid models (Arnold et al., 2020; Blöcker et al., 2016; Rubin et al., 2015).

Figure 3 displays the energy distributions of the electron fluxes within the LC before, during, and after selected crossings of the Europa footprint tail. In the near tail, the electron distribution appears as non-monotonic spectra, with a bump in the distribution (Figure 3a). These peaks, which increase almost linearly with energy, were identified as an indication of partially electrostatic acceleration during PJ12N by Allegrini et al. (2020). Further down in the tail, broadband spectra dominate (Figure 3c). The spectrum of PJ32S (Figure 3b) appears to be at the transition between the two regimes, with a spectrum that is mainly broadband but also contains two bumps. The spectra for the crossings not displayed in Figure 3 are provided in Figure S2 in Supporting Information S1.

#### 4. Discussion

We unambiguously identified 10 crossings of the Europa magnetic shell for which the JADE-E experiment onboard Juno observed electrons accelerated by the Europa-magnetosphere interaction. For each of these crossings, we calculated the downward electron EF and organized the results as a function of the angular separation

between the footprints of Juno and Europa. The  $\Delta\lambda_{\text{Alfvén}}$  metric, based on estimates of the Alfvén waves path between Europa and Jupiter's upper atmosphere is the best way to organize the downward EF with the downtail extent, as already shown by Szalay et al. (2020b) for Io. We derived e-folding values of  $7.4^\circ$  in good agreement with the values calculated by Bonfond, Saur, et al. (2017). This study used Hubble Space Telescope observations and the theoretical formalism of Hill and Vasyliūnas (2002) to estimate e-folding values of  $14^\circ$  and  $6^\circ$ , respectively. We point out that this theoretical model has been applied to a steady-state current system whereas our observations of moon-magnetosphere at Europa suggest wave-like interactions.

We emphasize that estimated e-folding value of the UV brightness, that is,  $14^\circ$ , is a factor of 2 higher than the e-folding of the observed downward EF. Such an observation was also made for Io, for which Szalay et al. (2020b) derived an e-folding value of  $21^\circ$  for the observed downward EF while the estimated e-folding value of the UV brightness is  $40^\circ$  (Bonfond, Saur, et al., 2017). This difference of values now reported at both Io and Europa could indicate that the energy transfer between waves and particles is more efficient than previously thought, leading to faster wave damping and shorter e-folding distances.

We point out that the computation of the  $\Delta\lambda_{\text{Alfvén}}$  separation is based on a statistical study of Europa's equatorial lead angle as a function of the moon's position in the plasma sheet. Temporal and spatial variations of the plasma density in the magnetodisk may lead to uncertainties of  $\sim 2\text{--}3^\circ$  in the  $\Delta\lambda_{\text{Alfvén}}$  separations, accounting for the low negative values for PJ13N and PJ23S. However, for PJ12N, the angular separation,  $\Delta\lambda_{\text{Alfvén}} = -11.4^\circ$ , is too large to be explained by these uncertainties. The negative separation suggests that Juno has crossed a structure upstream of the MAW, which could be the TEB.

We derived the size of the interaction region considering the magnetic projection of Juno's position in Europa's orbital plane at the beginning and the end of each crossing. Our calculation shows that this size is nearly the same in the near and far tail (Figure 2f), which means that the footprint tail does not widen.

We found two types of electron distributions, depending on the downtail distance. In the near tail, the spectra are non-monotonic and exhibit a peak in the electron distribution. Conversely, in the far tail, the spectra are mainly broadband. Future work may contrast this behavior with theoretical studies (Coffin et al., 2022; Damiano et al., 2019) to figure out how the Juno measurements challenge our understanding of electron acceleration associated with moon-magnetosphere interactions.

The statistical study of the Io-magnetosphere interaction conducted by Szalay et al. (2020b) shows that the downward EF also decays exponentially with the downtail extent. The e-folding value derived by their calculation is much larger (i.e.,  $21^\circ$ ) than at Europa, consistent with the longer auroral tail observed in UV. This lowest e-folding value for Europa might be also consistent with the propagation of Alfvén waves between Europa and Jupiter, which have a considerably larger distance to travel during each bounce, and may therefore be more rapidly attenuated (Jacobsen et al., 2007). The energy range of the accelerated electron is nearly the same at Io and Europa, with most of the particles having energies between 0.3 and 30 keV. In both cases, the characteristic energy of electrons tends to decrease with the distance in the tail (Figure 2e). However, the Io-magnetosphere interaction exhibits different features in terms of electron distributions, with broadband spectra appearing in both the near and far tail (Szalay et al., 2018, 2020b; Szalay, Bagenal, et al., 2020). In addition, unlike Europa, the size of the interaction region in Io's orbital plane was reported to increase with the downtail distance (Szalay et al., 2020b).

A statistical study of Ganymede-magnetosphere interaction remains to be conducted. There are, however, indications for Alfvénic acceleration in the MAW (Louis et al., 2020; Szalay et al., 2020a) which may also leave a broadband signature in the TEB (Hue et al., 2022). The possible diversity of electron acceleration processes at Io, Europa, and Ganymede, may result from not only the different upstream plasma conditions at  $M = 6$ ,  $M = 9$ , and  $M = 15$ , but also from the distinct characteristics of the Galilean moon obstacles, including the dense ionosphere of Io and the intrinsic magnetic field of Ganymede.

## 5. Conclusions

We characterized the properties of precipitating electrons measured during 10 crossings of the magnetic shell of Europa thanks to a joint analysis of Juno in situ and remote sensing measurements. The main results of this study are as follows:

1. The downward electron energy fluxes decay exponentially with distance along the auroral tail, with a mean e-folding value of  $7.4^\circ$ .



2. Two types of electron distribution exist, with non-monotonic energy spectra in the near tail and mainly broadband energy spectra in the far tail. The exact underlying acceleration mechanisms remain to be elucidated.
3. The estimated size of the interaction region is  $4.2 \pm 0.9 R_{\text{Eu}}$ , which is in good agreement with previous estimates based on theory and UV observations of the size of the footprint.
4. The size of the interaction region is the same in the MAW and in the tail, implying that the tail does not widen along its main direction.

## Data Availability Statement

JADE data used in this study are publicly available on the Planetary Data System, node Planetary Plasma Interactions website (PDS-PPI), in the dataset JNO-J/SW-JAD-3-CALIBRATED-V1.0 (<https://doi.org/10.17189/1519715>). UVS data are archived on the Atmospheres node (PPI-ATM). Part of the analysis have been done by the AMDA software (<http://amda.cdpp.eu>) provided by CDPP (<http://www.cdpp.eu/>) and the CLWEB software (<http://clweb.irap.omp.eu>) developed by E. Penou at IRAP.

## Acknowledgments

We are grateful to NASA and contributing institutions that have made the Juno mission possible. French authors acknowledge the support of CNES to the Juno mission. The work at SwRI was funded by the NASA New Frontiers Program for Juno through contract NNM06AA75C.

## References

- Allegri, F., Gladstone, G. R., Hue, V., Clark, G., Szalay, J. R., Kurth, W. S., et al. (2020). First report of electron measurements during a Europa footprint tail crossing by Juno. *Geophysical Research Letters*, *47*(18), e2020GL089732. <https://doi.org/10.1029/2020GL089732>
- Arnold, H., Liuzzo, L., & Simon, S. (2020). Plasma interaction signatures of plumes at Europa. *Journal of Geophysical Research: Space Physics*, *125*(1), e2019JA027346. <https://doi.org/10.1029/2019JA027346>
- Bigg, E. (1964). Influence of the satellite Io on Jupiter's decametric emission. *Nature*, *203*(4949), 1008–1010. <https://doi.org/10.1038/2031008a0>
- Blöcker, A., Saur, J., & Roth, L. (2016). Europa's plasma interaction with an inhomogeneous atmosphere: Development of Alfvén winglets within the Alfvén wings. *Journal of Geophysical Research: Space Physics*, *121*(10), 9794–9828. <https://doi.org/10.1002/2016JA022479>
- Bolton, S., Lunine, J., Stevenson, D., Connerney, J., Levin, S., Owen, T., et al. (2017). The Juno mission. *Space Science Reviews*, *213*(1), 5–37. <https://doi.org/10.1007/s11214-017-0429-6>
- Bonfond, B., Gladstone, G. R., Grodent, D., Greathouse, T. K., Versteeg, M. H., Hue, V., et al. (2017). Morphology of the UV aurorae Jupiter during Juno's first peri-jove observations. *Geophysical Research Letters*, *44*(10), 4463–4471. <https://doi.org/10.1029/2017GL073114>
- Bonfond, B., Grodent, D., Badman, S. V., Saur, J., Gérard, J.-C., & Radioti, A. (2017). Similarity of the Jovian satellite footprints: Spots multiplicity and dynamics. *Icarus*, *292*, 208–217. <https://doi.org/10.1016/j.icarus.2017.01.009>
- Bonfond, B., Grodent, D., Gérard, J.-C., Radioti, A., Saur, J., & Jacobsen, S. (2008). UV Io footprint leading spot: A key feature for understanding the UV Io footprint multiplicity? *Geophysical Research Letters*, *35*(5), L05107. <https://doi.org/10.1029/2007GL032418>
- Bonfond, B., Saur, J., Grodent, D., Badman, S., Bisikalo, D., Shematovich, V., et al. (2017). The tails of the satellite auroral footprints at Jupiter. *Journal of Geophysical Research: Space Physics*, *122*(8), 7985–7996. <https://doi.org/10.1002/2017JA024370>
- Clark, G., Tao, C., Mauk, B. H., Nichols, J., Saur, J., Bunce, E. J., et al. (2018). Precipitating electron energy flux and characteristic energies in Jupiter's main auroral region as measured by Juno/JEDI. *Journal of Geophysical Research: Space Physics*, *123*(9), 7554–7567. <https://doi.org/10.1029/2018JA025639>
- Clarke, J. T., Ballester, G. E., Trauger, J., Evans, R., Connerney, J. E., Stapelfeldt, K., et al. (1996). Far-ultraviolet imaging of Jupiter's aurora and the Io "footprint". *Science*, *274*(5286), 404–409. <https://doi.org/10.1126/science.274.5286.404>
- Coffin, D., Damiano, P., Delamere, P., Johnson, J., & Ng, C.-S. (2022). Broadband energization of superthermal electrons in Jupiter's inner magnetosphere. *Journal of Geophysical Research: Space Physics*, *127*(8), e2022JA030528. <https://doi.org/10.1029/2022JA030528>
- Connerney, J., Timmins, S., Herceg, M., & Joergensen, J. (2020). A Jovian magnetodisc model for the Juno era. *Journal of Geophysical Research: Space Physics*, *125*(10), e2020JA028138. <https://doi.org/10.1029/2020JA028138>
- Connerney, J. E. P., Baron, R., Satoh, T., & Owen, T. (1993). Images of excited H<sub>3</sub><sup>+</sup> at the foot of the Io flux tube in Jupiter's atmosphere. *Science*, *262*(5136), 1035–1038. <https://doi.org/10.1126/science.262.5136.1035>
- Connerney, J. E. P., Timmins, S., Oliverson, R. J., Espley, J. R., Joergensen, J. L., Kotsiaros, S., et al. (2022). A new model of Jupiter's magnetic field at the completion of Juno's prime mission. *Journal of Geophysical Research: Planets*, *127*(2), e2021JE007055. <https://doi.org/10.1029/2021JE007055>
- Damiano, P., Delamere, P., Stauffer, B., Ng, C.-S., & Johnson, J. (2019). Kinetic simulations of electron acceleration by dispersive scale Alfvén waves in Jupiter's magnetosphere. *Geophysical Research Letters*, *46*(6), 3043–3051. <https://doi.org/10.1029/2018GL081219>
- Gladstone, G. R., Persyn, S. C., Eterno, J. S., Walther, B. C., Slater, D. C., Davis, M. W., et al. (2017). The ultraviolet spectrograph on NASA's Juno mission. *Space Science Reviews*, *213*(1–4), 447–473. <https://doi.org/10.1007/s11214-014-0040-z>
- Hess, S., Bonfond, B., & Delamere, P. (2013). How could the Io footprint disappear? *Planetary and Space Science*, *89*, 102–110. <https://doi.org/10.1016/j.pss.2013.08.014>
- Hess, S., Delamere, P., Dols, V., Bonfond, B., & Swift, D. (2010). Power transmission and particle acceleration along the Io flux tube. *Journal of Geophysical Research*, *115*(A6), A06205. <https://doi.org/10.1029/2009JA014928>
- Hill, T. W., & Vasylunas, V. M. (2002). Jovian auroral signature of Io's corotational wake. *Journal of Geophysical Research*, *107*(A12), SMP27-1–SMP27-5. <https://doi.org/10.1029/2002JA009514>
- Hue, V., Gladstone, G. R., Louis, C. K., Greathouse, T. K., Bonfond, B., Szalay, J. R., et al. (2023). The Io, Europa and Ganymede auroral footprints at Jupiter in the ultraviolet: Positions and equatorial lead angles. *Journal of Geophysical Research: Space Physics*, e2023JA031363. <https://doi.org/10.1029/2023JA031363>
- Hue, V., Szalay, J. R., Greathouse, T. K., Bonfond, B., Kotsiaros, S., Louis, C. K., et al. (2022). A comprehensive set of Juno in situ and remote sensing observations of the Ganymede auroral footprint. *Geophysical Research Letters*, *49*(7), e2021GL096994. <https://doi.org/10.1029/2021GL096994>
- Jacobsen, S., Neubauer, F. M., Saur, J., & Schilling, N. (2007). Io's nonlinear MHD-wave field in the heterogeneous Jovian magnetosphere. *Geophysical Research Letters*, *34*(10), L10202. <https://doi.org/10.1029/2006GL029187>

- Louis, C. K., Louarn, P., Allegrini, F., Kurth, W. S., & Szalay, J. R. (2020). Ganymede-induced decametric radio emission: In situ observations and measurements by Juno. *Geophysical Research Letters*, *47*(20), e2020GL090021. <https://doi.org/10.1029/2020GL090021>
- Mauk, B. H., Haggerty, D. K., Paranicas, C., Clark, G., Kollmann, P., Rymer, A. M., et al. (2017). Juno observations of energetic charged particles over Jupiter's Polar Regions: Analysis of monidirectional and bidirectional electron beams. *Geophysical Research Letters*, *44*(10), 4410–4418. <https://doi.org/10.1002/2016GL072286>
- McComas, D., Alexander, N., Allegrini, F., Bagenal, F., Beebe, C., Clark, G., et al. (2017). The Jovian auroral distributions experiment (JADE) on the Juno mission to Jupiter. *Space Science Reviews*, *213*(1), 547–643. <https://doi.org/10.1007/s11214-013-9990-9>
- Prangé, R., Rego, D., Southwood, D., Zarka, P., Miller, S., & Ip, W. (1996). Rapid energy dissipation and variability of the Io–Jupiter electrodynamic circuit. *Nature*, *379*(6563), 323–325. <https://doi.org/10.1038/379323a0>
- Rubin, M., Jia, X., Altwegg, K., Combi, M., Daldorff, L., Gombosi, T., et al. (2015). Self-consistent multifluid MHD simulations of Europa's exospheric interaction with Jupiter's magnetosphere. *Journal of Geophysical Research: Space Physics*, *120*(5), 3503–3524. <https://doi.org/10.1002/2015JA021149>
- Saur, J. (2021). Overview of Moon–magnetosphere interactions. In *Magnetospheres in the solar system* (pp. 575–593). American Geophysical Union (AGU). <https://doi.org/10.1002/9781119815624.ch36>
- Szalay, J. R., Allegrini, F., Bagenal, F., Bolton, S. J., Bonfond, B., Clark, G., et al. (2020b). A new framework to explain changes in Io's footprint tail electron fluxes. *Geophysical Research Letters*, *47*(18), e2020GL089267. <https://doi.org/10.1029/2020GL089267>
- Szalay, J. R., Allegrini, F., Bagenal, F., Bolton, S. J., Bonfond, B., Clark, G., et al. (2020a). Alfvénic acceleration sustains Ganymede's footprint tail aurora. *Geophysical Research Letters*, *47*(3), e2019GL086527. <https://doi.org/10.1029/2019GL086527>
- Szalay, J. R., Bagenal, F., Allegrini, F., Bonfond, B., Clark, G., Connerney, J. E. P., et al. (2020). Proton acceleration by Io's Alfvénic interaction. *Journal of Geophysical Research: Space Physics*, *125*(1), e2019JA027314. <https://doi.org/10.1029/2019JA027314>
- Szalay, J. R., Bonfond, B., Allegrini, F., Bagenal, F., Bolton, S., Clark, G., et al. (2018). In situ observations connected to the Io footprint tail aurora. *Journal of Geophysical Research: Planets*, *123*(11), 3061–3077. <https://doi.org/10.1029/2018JE005752>
- Zarka, P. (1998). Auroral radio emissions at the outer planets: Observations and theories. *Journal of Geophysical Research*, *103*(E9), 20159–20194. <https://doi.org/10.1029/98JE01323>